JUSTC

Article

http://justc.ustc.edu.cn

Received: October 27, 2021; Accepted: January 04, 2022

Sheared $\boldsymbol{E} \times \boldsymbol{B}$ flow encountered in space plasma excited from two controllable methods

Kexin Huang[1], Xiao Zhang[1], Rong Jin[1], Yu Liu[1,2] ✉, and Jiuhou Lei[1,2]

[1]*CAS Key Laboratory of Geospace Environment, School of Earth and Space Sciences, University of Science and Technology of China, Hefei 230026, China;*
[2]*CAS Center for Excellence in Comparative Planetology, Hefei 230026, China*

✉*Correspondence: Yu Liu, E-mail: yliu001@ustc.edu.cn*

Graphical abstract

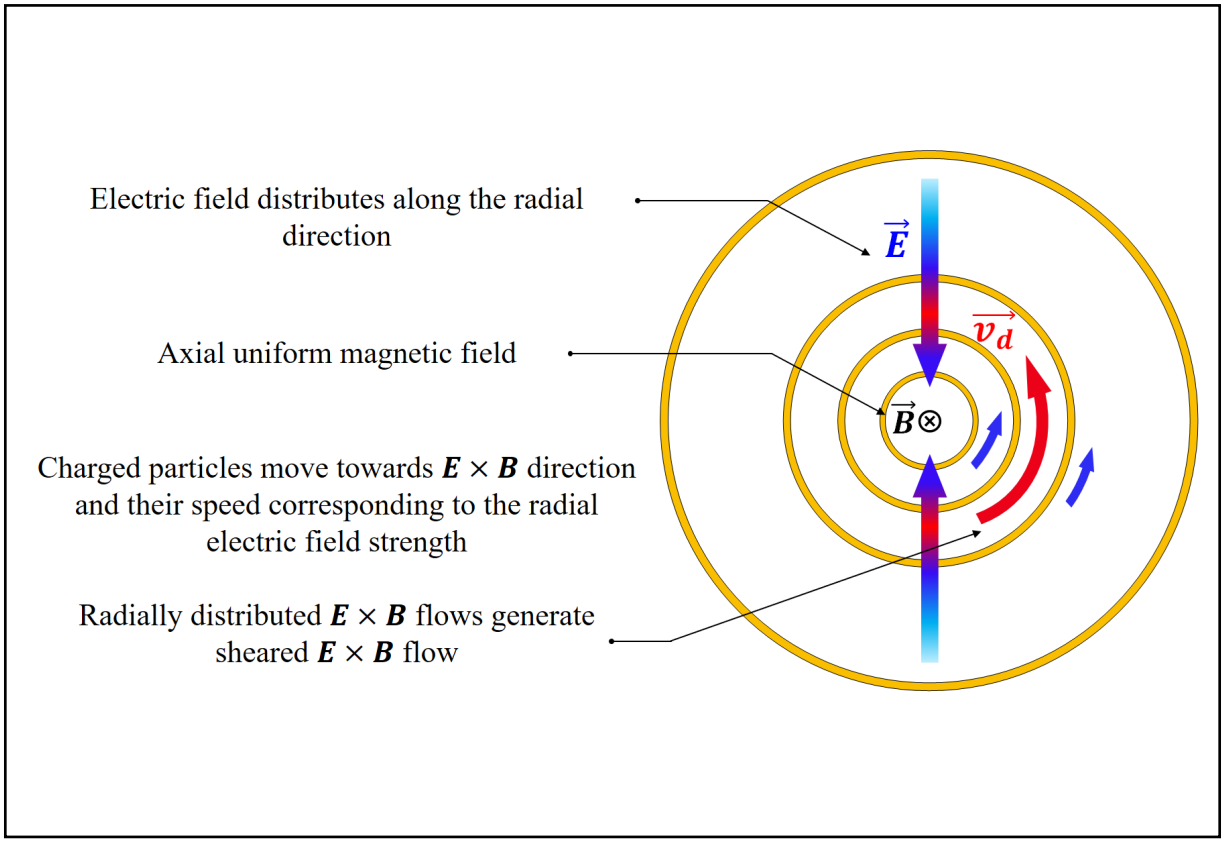

With the electric field varying along the radial position, the corresponding $\boldsymbol{E}\times\boldsymbol{B}$ *flow in different strengths yield sheared* $\boldsymbol{E}\times\boldsymbol{B}$ *flow.*

Public summary

- Sheared plasma flow is one of the most common free energy sources in ionospheric plasma for growing various instabilities which will further yield ionospheric irregularities and affect radio communicating system.
- The interpenetrating plasma method and ring electrode method have been presented in our work to generate a controllable sheared $\boldsymbol{E}\times\boldsymbol{B}$ flow.
- Plasma wave modes caused by sheared $\boldsymbol{E}\times\boldsymbol{B}$ flow are successfully generated which builds foundation for flowing experiments on ionospheric irregularities.

Citation: Huang K X, Zhang X, Jin R, et al. Sheared $\boldsymbol{E} \times \boldsymbol{B}$ flow encountered in space plasma excited from two controllable methods. *JUSTC*, **2022**, 52(2): 4. DOI: 10.52396/JUSTC-2021-0228

JUSTC

Article

http://justc.ustc.edu.cn

Received: October 27, 2021; Accepted: January 04, 2022

Sheared $\boldsymbol{E} \times \boldsymbol{B}$ flow encountered in space plasma excited from two controllable methods

Kexin Huang[1], Xiao Zhang[1], Rong Jin[1], Yu Liu[1,2] ✉, and Jiuhou Lei[1,2]

[1]*CAS Key Laboratory of Geospace Environment, School of Earth and Space Sciences, University of Science and Technology of China, Hefei 230026, China;*
[2]*CAS Center for Excellence in Comparative Planetology, Hefei 230026, China*

✉*Correspondence: Yu Liu, E-mail: yliu001@ustc.edu.cn*

Cite This: *JUSTC*, **2022**, 52(2): 4 (6pp)

Read Online

SI Supporting Information

Abstract: Sheared $\boldsymbol{E} \times \boldsymbol{B}$ flow has been frequently observed to excite instability in space plasma. In this study, two methods – the interpenetrating plasma and ring electrode methods – were developed in the Keda Space Plasma EXperiment (KSPEX) device to trigger sheared $\boldsymbol{E} \times \boldsymbol{B}$ flow. Both methods produce sheared $\boldsymbol{E} \times \boldsymbol{B}$ flow by generating a radial electric field. The results of the experiment indicated that plasma instabilities in the ion cyclotron range can be excited by these methods. Therefore, the methods reported here are important for research on the mechanism for generating sheared flow-driven plasma instabilities, which may enrich our understanding of geospace physics.

Keywords: sheared $\boldsymbol{E} \times \boldsymbol{B}$ flow; radial electric field; biasing electrode; ionospheric irregularities

CLC number: P354.4; O534 **Document code:** A

1 Introduction

Ionospheric irregularities can cause severe problems, such as ionospheric scintillation[1], that impacts radio communication and remote sensing. Thus, an in-depth study on the characteristics and the mechanisms by which these irregularities are generated is crucial[2–4]. The generation of the ionosphere irregularities can be attributed to various factors, such as altitudinal variations in ionospheric conductivity, neutral wind, and plasma instabilities[5]. Among these, plasma instabilities are widely considered to play an essential role in generating ionospheric irregularities[6, 7]. The mechanisms of many ionospheric physical processes can be linked to plasma instabilities, which may alter the equilibrium state of space. However, the details of the mechanisms by which these are generated, and their processes, remain ambiguous.

In a controlled laboratory experiment, plasma instabilities can be artificially excited by various methods, such as an inhomogeneous electric field, and parameters can be precisely adjusted and detected. Laboratory experiments can help reveal the formation and evolution of ionospheric irregularities using in situ observations and theoretical studies[8]. Sheared $\boldsymbol{E} \times \boldsymbol{B}$ flow is one of the most familiar sources of free energy for ionospheric plasma instability excitation. Instabilities driven by sheared $\boldsymbol{E} \times \boldsymbol{B}$ flow are often considered potential candidates for generating ionospheric irregularities[9–11]. Broadband instabilities ranging from whistler to sub-ion cyclotron frequency ranges – such as the electron-ion hybrid (EIH)[12], inhomogeneous energy-density driven (IEDD)[13], and Kelvin-Helmholtz (KH) instabilities[14, 15] – can be excited by the sheared $\boldsymbol{E} \times \boldsymbol{B}$ flow. Biasing electrodes such as ring electrodes[16–19], solid plates, button electrodes[20, 21], and grid electrodes[22, 23] are powerful tools to control flow and shear in the laboratory. When a positive DC voltage is biased on an electrode, electrons in the plasma will first gather around its surface because of the faster thermal speed related to the ions. The resulting negative potential of the electrode surface accelerates ions toward the surface. Once the ion and electron flow balance is established, a potential difference will be formed around the electrode surface and an inhomogeneous electric field can be generated. This is the modulation process of the plasma potential. A similar process occurs when a negative bias voltage is applied, with ions attracted and electrons repelled. Combined with the background magnetic field, a sheared $\boldsymbol{E} \times \boldsymbol{B}$ flow can be formed in the plasma.

In this work, the interpenetrating plasma and ring electrode methods used to trigger sheared $\boldsymbol{E} \times \boldsymbol{B}$ flow by generating a radial electric field were studied in the laboratory. The sheared $\boldsymbol{E} \times \boldsymbol{B}$ flow can excite various instabilities according to the experimental parameters. Each method exhibits unique features and can be used to excite plasma instabilities responsible for ionospheric irregularities.

2 Experimental setup

Experiments were conducted using the Keda Space Plasma EXperiment (KSPEX) device[24]. Fig. 1 shows the sketch of the main parts of the experimental chamber, including a vacuum chamber, six magnet coils, and two plasma source chambers. The vacuum chamber is 2.73 m in length and 0.5 m in diameter and surrounded by six magnet coils that generate a uniform axial magnetic field ranging from 20 to 1000 G ($\delta \boldsymbol{B}/\boldsymbol{B} \approx 0.01$). According to the experimental conditions of these two methods, hot filament, an inductively coupled plasma (ICP), and large-area oxide-coated cathode sources can be chosen. Plasma was produced by ionizing argon gas at

DOI: 10.52396/JUSTC-2021-0228
JUSTC, **2022**, 52(2): 4

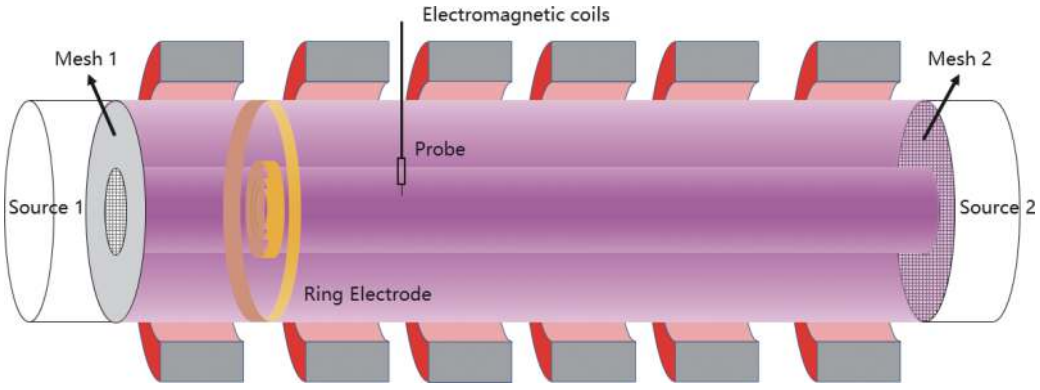

Fig. 1. Schematic of the plasma sources and two types of biasing electrodes applied to generate sheared $\boldsymbol{E} \times \boldsymbol{B}$ flow.

a desirable pressure of approximately 10^{-3}–10^{1} Pa. The distributions of plasma density and potential were determined using a radially movable Langmuir single probe and an emissive probe, respectively. Both probes were arranged at 110 cm downstream from the plasma source to avoid the influence of the electrode on the probe (as shown in Fig. 1). The corresponding electric field distributions were subsequently calculated from the gradient of the plasma potential. The axial and azimuthal potential fluctuations were also detected using a multiple-tip floating probe, where two tips were separated by a certain distance to detect the potential signals. The phase difference between these two signals gives the wavelength λ. The wave frequency f can be obtained by applying a fast Fourier transform (FFT) to the potential signals, and other information related to wave propagation can be calculated further using λ and f.

Different electrodes (the ring electrode and Mesh 1 and Mesh 2 shown in Fig. 1) were designed and installed to adjust the plasma potential. In the interpenetrating plasma method, primary plasma was produced by a hot filament source (Source 1) and secondary plasma was produced by an ICP source (Source 2). Two stainless meshes (Meshes 1 and 2) were specially designed to obtain an interpenetration plasma layer. The outer region of the plasma produced by Source 1 (primary plasma) was blocked by a Macor blocking disk on Mesh 1 (Fig. 2). The plasma emitted from Source 2 (secondary plasma) filled this void while the central portion of Mesh 2 was blocked. Each mesh was biased by a DC power supply by which the potential of the primary and secondary plasma to generate an inhomogeneous radial electric field could be controlled.

However, in some experiments, only one plasma source could be installed. Therefore, the method mentioned above was not suitable for this condition and a new method was designed and fabricated. A ring electrode, consisting of four concentric rings (Fig. 3), was designed to generate a radial electric field. The outermost ring was a holder connected to the chamber wall to maintain stabilization. The radii of the inner three rings were 8, 5, and 2.5 cm, respectively. The electrode was installed 1.3 m away from the plasma source (shown in Fig. 1). Each ring was electrically isolated via machinable ceramics and biased by a DC power supply ranging from 0 to 300 V to independently regulate the distribution of plasma potential. The plasma column was compressed to a smaller radius by the magnetic field (14 cm for the interpenetrating plasma method and 8 cm for the ring electrode method). The radius of the plasma is smaller than that of the vacuum chamber (25 cm); therefore, the boundary effect can be ignored in this study.

Fig. 2. Mesh 1 and Mesh 2 used to bias two plasma layers.

Fig. 3. Ring electrode designed to modulate the distribution of plasma potential.

3 Results and discussions

In the interpenetrating plasma method, the radial electric field can be modulated by adjusting the potential difference between the primary and secondary plasmas. Mesh 2 was electrically grounded to ensure that the potential of the secondary plasma would not float randomly. Thus, a potential difference could be achieved by regulating the biasing voltage of Mesh 1. The resultant profiles of the plasma potential and electric field are shown in Fig. 4a, with Mesh 1 biased at 120 V. The average plasma potential of the primary plasma was approximately 120 ± 2.3 V, which equaled the DC biasing voltage. The secondary plasma potential was approximately 53 ± 2.4 V. A sheared region was formed at the position corresponding to the interpenetrating region, which is marked in gray in Fig. 4a. The "sheared region" denotes the boundary layer between the two types of plasma with different electron

DOI: 10.52396/JUSTC-2021-0228
JUSTC, **2022**, 52(2): 4

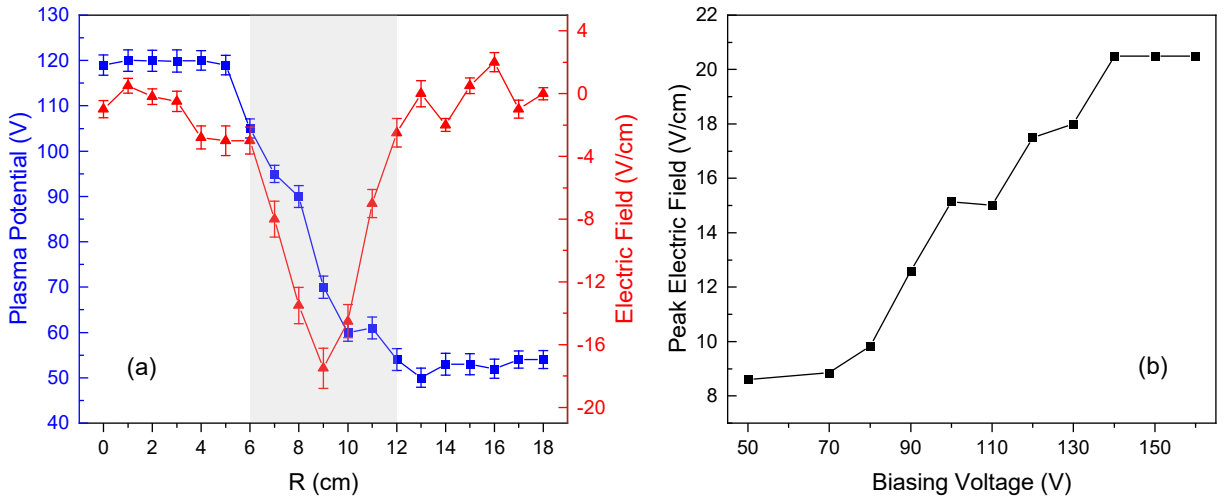

Fig. 4. (a) Radial profiles of the plasma potential and the electric field with Mesh 1 biased at 120 V and Mesh 2 grounded. The grey shaded area denotes the sheared region. (b) The electric field peak value versus varying biasing voltage on Mesh 1.

drift velocities, i.e., two radial electric field strengths. The shear strength is given by $V_d' = \mathrm{d}v_d/\mathrm{d}r$ [25]. The electric field maximum appears, here, to be about $17.5 \pm 1.3\ \mathrm{V \cdot cm^{-1}}$ with the scale length $L_E = \left(\frac{1}{E}\frac{\mathrm{d}E}{\mathrm{d}r}\right)^{-1} \approx 0.9 \pm 0.1$ cm. Fig. 4b shows that the peak value of the electric field increases from $8.6\ \mathrm{V \cdot cm^{-1}}$ to $20.5\ \mathrm{V \cdot cm^{-1}}$ as the biasing voltages applied on Mesh 1 vary from 50 V to 160 V. This indicates that the shearing strength can be regulated by changing the biasing voltage. The electrostatic fluctuation in the ion cyclotron frequency range excited by inhomogeneous energy-driven instability (IEDDI) was investigated using the interpenetrating plasma method, whose peak frequency was as low as $\omega \approx 0.3\omega_{ci}$, where ω_{ci} is the ion cyclotron frequency. This is a unique result because previous experiments could not produce such a low-frequency IEDDI[26].

Regarding the ring electrode method, the inner ring was biased to a negative potential, and the two outer rings were connected and biased at 10 V to the ground to achieve a stable plasma condition. Plasma potential was measured using an emissive probe. Fig. 5a shows the radial distributions of the plasma potential and the electric field when the inner ring was biased at –30 V and the outer rings were biased at 10 V. The plasma potential at the boundary region is higher and almost equals the bias voltage (~10 V). There is an apparent sheared region where a potential drop exists between the inner and the middle rings. A corresponding electric field is subsequently produced, and the peak value is about $1.55 \pm 0.67\ \mathrm{V \cdot cm^{-1}}$ with a scale length $L_E = \left(\frac{1}{E}\frac{\mathrm{d}E}{\mathrm{d}r}\right)^{-1} \approx 0.45 \pm 0.1$ cm. The plots provide the distribution of the $R > 0$ cm region because the probe holder needs to traverse half the plasma column to measure the opposite part. This will lead to a significant electrical disturbance and introduce extra errors. Fig. 5b shows the peak value of the electric field under different bias voltages. According to the profiles, when all the rings were floating (corresponding to "0 / 0" of the horizontal axis), no apparent radial electric field was generated. When the two

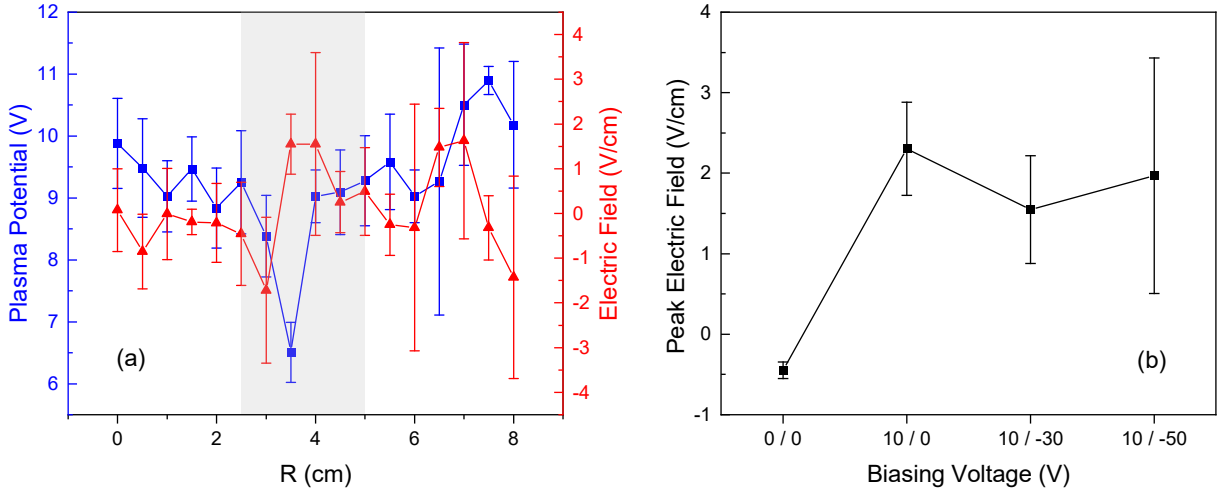

Fig. 5. (a) Radial profiles of the plasma potential and the electric field as the outer rings biased at 10 V and the inner ring biased at –30 V. The grey shaded area denotes the sheared region. (b) The electric field peak value versus different biasing voltages. The horizontal axis is in the format of "bias on the outer ring / bias on the inner ring" while "0 V" refers to electrical floating or electrical insulation. The background magnetic field was fixed at 130 G for all these cases.

DOI: 10.52396/JUSTC-2021-0228
JUSTC, **2022**, 52(2): 4

outer rings were fixed at 10 V, the electric field peak varied slightly regardless of the bias of the inner ring and was approximately 2 $\mathrm{V \cdot cm^{-1}}$.

As shown in Figs. 4b and 5b, the electric field peaks do not change after the bias voltage exceeds a threshold value. The collective effect of plasma plays a significant role in the response to an external electric field. The charged particles tend to weaken the impact of the external electric field. Therefore, the plasma potential is often inconsistent with the direct application of bias voltage. In addition, considering the finite charged particle number density, the ability of plasma to respond to the external electric field has a certain threshold. Both of these lead to the results shown in Figs. 4b and 5b. The average level of the error bars in Figs. 4a and 5a are close to and within the error margin (1.480 V for plasma potential and 0.986 $\mathrm{V \cdot cm^{-1}}$ for the electric field, respectively), which indicates that both methods can control the potential with a high accuracy.

Fig. 6 shows the radial profile of the electric field distribution under two different magnetic field conditions. When the magnetic field strength was set to 40 G, the peak value of the electric field reached approximately 4 $\mathrm{V \cdot cm^{-1}}$. The magnitude of the electric field decreased by almost half (2 $\mathrm{V \cdot cm^{-1}}$) when the magnetic field strength was increased to 130 G. This suggests that the peak value of the electric field decreases as the magnetic field increases, and the electric field scale length shrinks under the strengthened magnetic field. This was attributed to the frozen effect of the plasma. The stronger magnetic field squeezes the plasma into a smaller column and weakens the perpendicular mobility of the charged particles.

Plasma perturbation induced by an inhomogeneous electric field was simultaneously detected using multiple-tip floating probe. The power spectrum density（PSD）of the potential fluctuation varying with different bias voltages was calculated using FFT and plotted in Fig. 7. Fig. 7a shows that no plasma wave mode was excited when all the ring electrodes were floating. When a 10 V voltage was biased on the outer

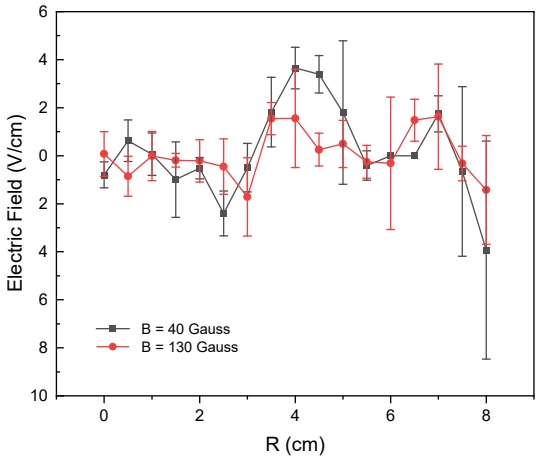

Fig. 6. Radial profiles of the electric field distribution under two different magnetic field strengths.

rings, the plasma waves were excited by the sheared $\boldsymbol{E} \times \boldsymbol{B}$ flows, whose frequencies were approximately 2, 4, and 6 kHz, as well as other weak harmonic waves. Three similar wave modes can also be observed when the DC voltage on the inner ring varied from −10 V to −70 V. The fundamental frequency and magnitude under biasing voltages changed slightly (Fig. 7b), but an additional $\boldsymbol{E} \times \boldsymbol{B}$ doppler shift could be seen when compared to the case of "10 / 0 V" (Fig. 7a). This can be ascribed to the almost unchanged or slightly changed electric field (as shown in Fig. 5b) under different inner-ring biasing voltages. Identifying the plasma wave modes is a complex issue, and more diagnostic information is required. Thus, the characteristics of plasma waves will be discussed in detail in our future work.

4 Conclusions

In this study, two controllable methods for triggering sheared $\boldsymbol{E} \times \boldsymbol{B}$ flows were investigated. The interpenetrating plasma method generated a sheared $\boldsymbol{E} \times \boldsymbol{B}$ flow through two-ended plasma sources and two mesh electrodes. The plasma potential

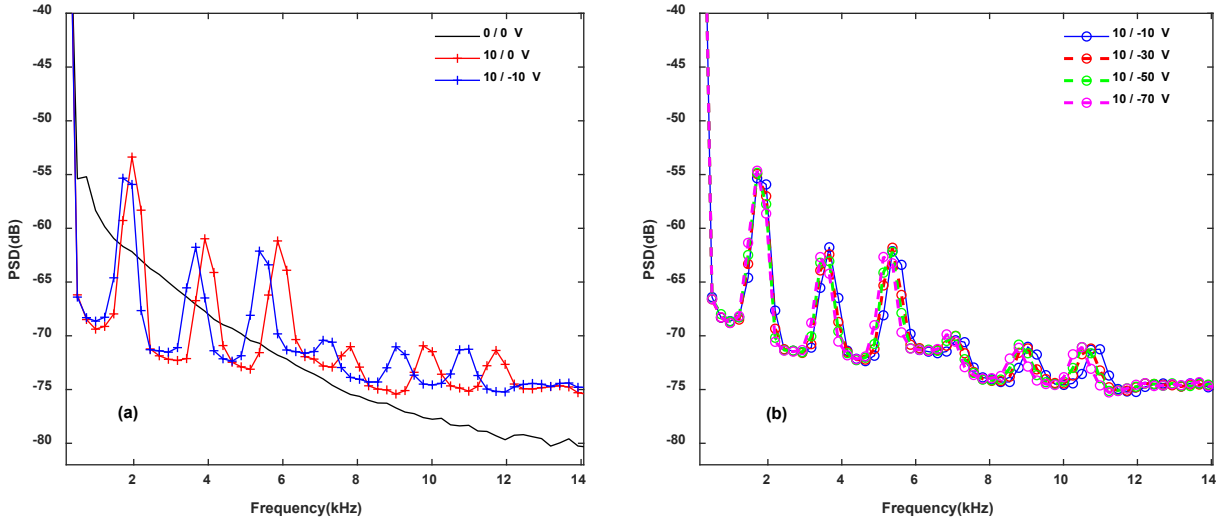

Fig. 7. PSD of potential fluctuation versus different biasing voltages on the ring electrodes. The legend is written in the format of "bias on the outer ring / bias on the inner ring" while "0 V" refers to electrical floating or electrical insulation. The magnetic field strength was fixed at 130 G, and the radial position was fixed at 4 cm.

DOI: 10.52396/JUSTC-2021-0228
JUSTC, **2022**, 52(2): 4

profile could be adjusted by varying the bias voltages on the meshes, and the sheared $\boldsymbol{E} \times \boldsymbol{B}$ flow could be excited within the interpenetrating region. When Mesh 1 was biased to 120 V and Mesh 2 is grounded, the electric field maximum was approximately $17.5 \pm 1.3\ \mathrm{V \cdot cm^{-1}}$ with the scale length $L_E = \left(\frac{1}{E}\frac{\mathrm{d}E}{\mathrm{d}r}\right)^{-1} \approx 0.9 \pm 0.1$ cm (as shown in Fig. 4a). The peak electric field increased as the biasing voltage on Mesh 1 varied from 50 V to 160 V in intervals of 10 V, but became constant beyond 120 V biasing. This approach could produce a considerable plasma potential gradient; therefore, it would be appropriate for situations requiring a large radial electric field. However, the experimental setup was relatively complex, and the ceramic-supported Macor disk on the mesh electrode was fragile under high-temperature conditions. The ring electrode method was designed to avoid these shortcomings and only one plasma source was required, with the latter greatly simplifying the experimental configuration. This method benefits conditions when no additional ports are available for installing another plasma source or plasma sources are insufficient. In previous studies, similar electrodes were used to modulate the plasma potential, but most of them were biased as a whole[27, 28]; therefore the distribution of the electric field was not controllable.

However, in our work, an independent-biasing improvement was made to allow a controllable inhomogeneous electric field profile. As shown in Fig. 5a, when the outer two rings are connected and biased to 10 V, and the inner ring is biased to −30 V, an inhomogeneous electric field with the maximum of $1.55 \pm 0.67\ \mathrm{V \cdot cm^{-1}}$ and the scale length $L_E = \left(\frac{1}{E}\frac{\mathrm{d}E}{\mathrm{d}r}\right)^{-1} \approx 0.45 \pm 0.1$ cm was produced successfully using our method. As the sheared $\boldsymbol{E} \times \boldsymbol{B}$ flows were excited, plasma waves were also detected from the potential fluctuation with frequencies of approximately 2, 4, and 6 kHz, and other weak harmonic waves. Detailed analysis of the sheared-driven wave modes will be conducted in our following work. Our results demonstrated that the ring electrode method was reliable and could be extended to investigate shear-driven instabilities that account for ionospheric irregularities. However, the adjusting range of the radial electric field is limited due to the collective effect of plasma especially for the ring electrode method which may reduce its availability. We will improve the methods in subsequent experiments. In spite of sheared $\boldsymbol{E} \times \boldsymbol{B}$ flow, these two methods also show great application in experiments where a background electric field is needed. This enable researches on instability caused by other sources of free energy to be carried on.

Acknowledgements

This work is supported by the USTC Research Funds of the Double First-Class Initiative (YD3420002002), the Youth Innovation Promotion Association CAS (2020451) and Fundamental Research Funds for the Central Universities (WK3420000011).

Conflict of interest

The authors declare that they have no conflict of interest.

Biographies

Kexin Huang is currently a graduate student under the tutelage of Associate Professor Yu Liu at the University of Science and Technology of China. Her research interests focus on laboratory experiments on instability processes encountered in ionosphere of Earth.

Yu Liu received his BS degree in Physics from Nanyang Normal University, Nanyang, China, in 2009, and his PhD degree in Plasma Physics from the University of Science and Technology of China (USTC), Hefei, China, in 2015. He is an associate professor with the School of Earth and Space Sciences, USTC. His research interests include the laboratory study of partially ionized plasma physics and their applications to ionospheric research.

References

[1] Makarevich R A, Crowley G, Azeem I, et al. Auroral *E*-region as a source region for ionospheric scintillation. *Journal of Geophysical Research:Space Physics,* **2021**, *126* (5): e2021JA029212.
[2] Hysell D L. From instability to irregularities. In: The Dynamical Ionosphere. Amsterdam, Netherlands: Elsevier, 2020: 137-167.
[3] Fejer B G, Kelley M C. Ionospheric irregularities. *Reviews of Geophysics,* **1980**, *18* (2): 401–454.
[4] Wernik A W, Secan J A, Fremouw E J. Ionospheric irregularities and scintillation. *Advances in Space Research,* **2003**, *31* (4): 971–981.
[5] Balsley B B, Ecklund W L. VHF power spectra of the radar aurora. *Journal of Geophysical Research,* **1972**, *77* (25): 4746–4760.
[6] Kintner P, D'Angelo N. A transverse Kelvin-Helmholtz instability in a magnetized plasma. *Journal of Geophysical Research,* **1977**, *82* (10): 1628–1630.
[7] Pradhan S M, Tiwari R S, Singh B, et al. Ionospheric irregularities plasma instability. *Indian Journal of Radio Space Physics,* **1972**, *1*: 218–220.
[8] Liu Y, Shi P, Zhang X, et al. Laboratory plasma devices for space physics investigation. *Review of Scientific Instruments,* **2021**, *92* (7): 071101.
[9] Ganguli G, Keskinen M J, Romero H, et al. Coupling of microprocesses and macroprocesses due to velocity shear: An application to the low-altitude ionosphere. *Journal of Geophysical Research:Space Physics,* **1994**, *99* (A5): 8873–8889.
[10] Linson L M, Workman J B. Formation of striations in ionospheric plasma clouds. *Journal of Geophysical Research,* **1970**, *75* (16): 3211–3219.
[11] Tsuda T, Sato T, Matsushita S. Ionospheric irregularities and the cross-field plasma instability. *Journal of Geophysical Research,* **1969**, *74* (11): 2923–2932.
[12] Ganguli G, Lee Y C, Palmadesso P J. Electron–ion hybrid mode due to transverse velocity shear. *The Physics of Fluids,* **1988**, *31* (10): 2753–2756.
[13] Ganguli G, Lee Y C, Palmadesso P J. Kinetic theory for electrostatic waves due to transverse velocity shears. *The Physics of Fluids,* **1988**, *31* (4): 823–838.
[14] Nykyri K, Otto A. Plasma transport at the magnetospheric boundary due to reconnection in Kelvin-Helmholtz vortices. *Geophysical Research Letters,* **2001**, *28* (18): 3565–3568.
[15] Johnson J R, Wing S, Delamere P A. Kelvin Helmholtz instability in planetary magnetospheres. *Space Science Reviews,* **2014**, *184* (1-4): 1–31.
[16] Jassby D L. Transverse velocity shear instabilities within a magnetically confined plasma. *The Physics of Fluids,* **1972**, *15* (9): 1590–1604.
[17] Thomas Jr E, Jackson J D, Wallace E A, et al. Observations of low

DOI: 10.52396/JUSTC-2021-0228
JUSTC, **2022**, 52(2): 4

frequency oscillations due to transverse sheared flows. *Physics of Plasmas,* **2003**, *10* (5): 1191–1194.

[18] Amatucci W E, Koepke M E, Carroll III J J, et al. Observation of ion-cyclotron turbulence at small values of magnetic-field-aligned current. *Geophysical Research Letters,* **1994**, *21* (15): 1595–1598.

[19] Yoshinuma M, Inutake M, Hatakeyama R, et al. Control of radial potential profile and related low-frequency fluctuations in an ECR-produced plasma. *Physics Letters A,* **1999**, *255* (4–6): 301–306.

[20] D'Angelo N. Kelvin-Helmholtz instability in a fully ionized plasma in a magnetic field. *The Physics of Fluids,* **1965**, *8* (9): 1748–1750.

[21] Teodorescu C, Reynolds E W, Koepke M E. Observation of inverse ion-cyclotron damping induced by parallel-velocity shear. *Physical Review Letters,* **2002**, *89* (10): 105001.

[22] Fujita H, Yagura S, Harada T, et al. Observation of potential relaxation instability in a bounded discharge plasma. *IEEE Transactions on Plasma Science,* **1987**, *15* (4): 445–451.

[23] Kaneko T, Odaka Y, Tada E, et al. Generation and control of field-aligned flow velocity shear in a fully ionized collisionless plasma. *Review of Scientific Instruments,* **2002**, *73* (12): 4218–4222.

[24] Liu Y, Zhang Z, Lei J, et al. Design and construction of Keda Space Plasma Experiment (KSPEX) for the investigation of the boundary layer processes of ionospheric depletions. *Review of Scientific Instruments,* **2016**, *87* (9): 093504.

[25] Kaneko T, Tsunoyama H, Hatakeyama R. Drift-wave instability excited by field-aligned ion flow velocity shear in the absence of electron current. *Physical Review Letters,* **2003**, *90* (12): 125001.

[26] Liu Y, Lei J, Yu P, et al. Laboratory generation of broadband ELF waves by inhomogeneous plasma flow. *Geophysical Research Letters,* **2017**, *44* (4): 1634–1640.

[27] D'Angelo N, Pécseli H L, Petersen P I. The Farley instability: A laboratory test. *Journal of Geophysical Research,* **1974**, *79* (31): 4747–4751.

[28] Desjardins T R, Gilmore M. Dynamics of flows, fluctuations, and global instability under electrode biasing in a linear plasma device. *Physics of Plasmas,* **2016**, *23* (5): 055710.

DOI: 10.52396/JUSTC-2021-0228
JUSTC, **2022**, 52(2): 4